CHAPTER VI
PREPARATION AND CHARACTERIZATION OF HIGH-THERMAL STABILITY COPPER-CERIA-ZIRCONIA-ALUMINA CATALYST PREPARED BY SOL-GEL PROCESS AND ITS REDUCTION PROPERTY

6.1 Abstract

This work is focused on copper-ceria-zirconia-alumina mixed oxides prepared through a surfactant-aid sol gel method at room temperature. The amount of ceria:zirconia is fixed at a 6:4 mole ratio, while the alumina amount is varied. The surface features, textural properties, and crystalline structures of the mixed oxides are studied by means of X-ray diffraction (XRD), Brunauer-Emmett-Teller specific surface areas measurement (BET) and temperature programmed reduction (TPR). The thermal stability of mixed oxides was examined. The XRD studies show that minor θ-alumina phase still exists in the samples with ≥20% Ce-Zr doping content after aging at 1100°C for 24 h. The best stabilizing effect is observed in the case of the sample with 20 wt% $Ce_{0.6}Zr_{0.4}O_2$. The Cu (25%)-CeO_2 (20 wt%)/Al_2O_3 catalyst showed the highest catalytic activity for the CO oxidation reaction at lower temperature, but the catalytic activity of Cu (25%)-CeO_2 (20 wt%)/Al_2O_3catalyst decreased more rapidly than that of Cu (25 mol%)-$Ce_{0.6}Zr_{0.4}O_2$ (20 wt%)/Al_2O_3 catalyst when the calcination temperature increased to 1100°C.

Keywords: Copper, Ceria, Zirconia, Aluminas, Sol-gel process, CO oxidation

6.2 Introduction

The three-way catalyst (TWC), capable of converting, under proper stoichiometric air-to-fuel ratio (A/F), CO and hydrocarbons (HC) to CO_2/H_2O, and, simultaneously, reducing NO_x to N_2, has been employed in automotive catalytic converters since 1980s[1]. The conventional TWCs mostly contained active noble Rh and Pt as active noble metals and CeO_2 as oxygen storage component.

As stringent quality standards for automotive emissions have been put in place by U.S. TIER 2 regulations[2], the development of more efficient catalysts for abatement of exhaust emissions is essential. In fact, a major problem of the TWC converters is that significant conversions are attained only at high temperatures (>600 K). As a result, during the cold-start of the engine, the emissions of the pollutants, particularly the HC, are quite high until the converter reaches the operating temperature. Accordingly, inclusion of the cold-start in the engine test and the remarkably low limits required in the near future for the HC emissions demanded for the development of the so-called close coupled catalyst (CCC).

The close coupled converter (CCC) is employed to improve efficiency (over 95-98% of pollutants conversion) of TWCs during cold start-up of the engine. This converter is mounted directly on the engine exhaust manifold, which exposes the catalyst to temperatures as high as 1173°C. Such high temperatures together with the required durability (over 120,000 miles) represent a strong challenge in the development of thermally stable catalytic materials.

A number of catalysts have been investigated in the past decades, supported noble metal catalysts have given promising results, because of their responsible activity, good hydrothermal and resistance to impurities such as SO_2[3]. However, the employment of noble metal catalysts is limited due to their scarce and high cost, and the substitution by the cheap metals for the noble metals has attracted much interest recently[4].

Copper-contained catalysts show a potential activity for the treatment of exhaust gas from automobiles and have been extensively investigated during the past decades[5]. During CO oxidation, copper-ceria mixed oxide catalysts can exhibit activities per unit surface area that are similar to those of noble-metal catalysts such

as platinum[6]. The promoting effect has been correlated with the synergism of the redox properties of the system, which is achieved by the formation of copper-ceria interactions, with both components being significantly more readily reduced or oxidized than the corresponding independent components[7].

Highest conversion of the pollutants in automotive catalytic converters is attained close to the stoichiometric conditions, while excursions to fuel-rich (net reducing) or fuel-poor (net oxidizing) air-to-fuel (A/F) ratios severely decrease the efficiency of the TWCs. Such excursions may represent a serious limitation for a TWC since the A/F significantly oscillates around the stoichiometric value A/F.14.6. Addition of CeO_2 limits this disadvantage due to its ability to act as an oxygen buffer by storing/releasing O_2 due to the Ce^{+4}/Ce^{+3} redox couple. Major drawback of ceria is its low stability in high temperature ranges, as a support its use will result in a significant efficiency decrease of the catalysts due to loss of surface area of the support, sintering of active metals and deactivation of ceria under thermally harsh environments[8].

A strong effort has been directed to increase the overall efficiency of CeO_2 in these applications. Many studies show the improvement of textural properties by introducing doping elements in the CeO_2 fluorite-type lattice, and the most efficient metal seem to be zirconia. Their effectiveness derives from the improvement of several features with respect to catalysts based on pure ceria: ceria-zirconia shows enhanced redox and oxygen storage properties[9] ; improved thermal resistance[10] ; and better catalytic activity at lower temperatures[11].

Nowadays, there is a general agreement that the presence of a single-phase solid solution is preferable compared to microdomain or phase-segregated non-homogeneous CeO_2-ZrO_2 mixed oxides, as the former systems generally lead to better textural stability and redox properties[12]. In addition to high activity and cost-effectiveness, durability is the most important property of a TWC; accordingly it is expected that a single-phase product should feature less modification during its lifetime in the converter.

Given the importance of the textural stability for practical application of the CeO_2-ZrO_2 in the TWCs, the design of nanocomposites where the CeO_2-ZrO_2 phase is dispersed over a stable inert support could represent a suitable way to improve

thermal stability of these systems. To date, relatively few papers have been devoted to this topic and only recently the effects of addition of Al_2O_3 on the thermal stability and reduction behavior of CeO_2-ZrO_2 mixed oxides have been reported[13-15].

There are some reasons that could account for the lack of extensive studies in this area. As observed above, the synthesis of the single phase CeO_2-ZrO_2 may be difficult, requiring appropriate synthesis strategies to be adopted. This clearly becomes even more important when a third component (Al_2O_3) is added.

Another important aspect is that while nano-dispersed CeO_2 particles could be obtained by impregnating Al_2O_3 with a $Ce(NO_3)_3$ precursor and subsequent calcination[16], this does not necessarily result in a good OSC promoter. As shown by detailed studies reported more than a decade ago, the intimate contact between Al_2O_3 and the highly dispersed CeO_2 particles, which is generated by the deposition process, favors formation of $CeAlO_3$ after high-temperature aging that deactivates the OSC component[17].

Consider the effect of Al_2O_3 addition to CeO_2-ZrO_2 mixed oxides. As in the case of unsupported mixed oxides, optimized synthesis procedures are needed to produce single-phase CeO_2-ZrO_2 products at the surface of Al_2O_3. Observation of a multiphase system can be attributed to either a phase segregation or presence of compositional non-homogeneities in the starting product. It is therefore difficult to assess the appropriateness of a synthesis methodology to produce a solid solution.

A perusal of the data reported in the literature shows that simple impregnation of Al_2O_3 with nitrates of ceria and zirconia is ineffective in producing homogeneous products, which apparently is due to the fact that ZrO_2 tends to spread as an amorphous layer over the surface of Al_2O_3[18]. Recently, a number of papers addressed the issue of CeO_2-ZrO_2-Al_2O_3 materials with the aim of improving the thermal stability and redox properties of the CeO_2-ZrO_2 mixed oxides, however, complex and expensive synthesis strategies had to be employed to achieve materials with a reasonably good structural homogeneity of the CeO_2-ZrO_2 mixed oxides and thermal stability of the system[19-20].

The aim of this present paper is to develop novel thermally stable nanocomposite materials based on Cu (25 mol%)-$Ce_{0.6}Zr_{0.4}O_2/Al_2O_3$ systems. The

effects of composition on the texture, structure, redox properties, catalytic activity for CO oxidation and thermal stability of the samples are also evaluated.

6.3 Experimental

6.3.1 Materials

Cerium(IV)hydroxide, zirconium(IV)hydroxide, $Cu(CH_3COO)_2 .H_2O$, and sodium dodecyl sulfate were purchased from Aldrich Chemical Co. Inc. (USA) and used as received. Aluminium hydroxide hydrate ($Al(OH)_3$) was purchased from Sigma Chemical Co., and TIS was obtained from Fluka Chemical Co. Both were used as received. Ethylene glycol was purchased from Farmitalia Carlo Erba (Barcelona), and sodium hydroxide was purchased from Merck Company Co. Ltd. (Germany), and used as received. Triethylenetetramine was purchased from Facai Polytech. Co. Ltd. (Bangkok, Thailand) and distilled under vacuum (0.1 mm Hg) at 130°C prior to use.

6.3.2 Instruments

The structure of the samples was investigated from the wide-angle X-ray diffraction (XRD) on a D/MAX 2000 Rigaku using CuK_α radiation (λ = 1.5406 Å). The intensity data were collected at 25°C over a 2θ range of 5-90 degree.

Due to the small particle sizes, the XRD peaks were extensively broadened, and some peaks overlapped. Peak positions and widths were resolved by profile fitting. The average grain size (D) was estimated according to the Scherrer equation:

$$D = 0.94\lambda / \beta \cos\theta$$

where θ is the diffraction angle of the (111) peak of the cubic phase or the (101) peak of the tetragonal phase, and β is the full width at half-maximum (fwhm) of the (111) or the (101) peak (in radian).

The reduction properties of the catalysts were measured by temperature programmed reduction (TPR). A micromeritics TPD/TPR 2900 was employed as the analyzer for the temperatures of the thermal conductivity, using a furnace temperature up to 900°C at a linear ramp rate of 2.5°C/min. The sample was

pretreated by flowing He over the sample at 120°C for 4 h and then cooled to room temperature before analysis; 10 mg of the catalysts were used for each test. The reaction mixture was consisted of 5% H_2 in N_2. An effluent gas stream from the reactor was first dehumidified by a cold water-trap before auto-sampling in a gas chromatograph (Agilent Technologies 6890N model). The results were recorded by Agilent Chemstation software. The observed peaks were identified by comparison with the retention time of the standard gas.

The Brunauer-Emmett-Teller (BET) specific surface areas of all powder samples were determined by N_2 adsorption and desorption isotherms at 77K using a Quantachrome Corporation Autosorb. Prior to analysis, the samples were outgassed at 250°C for 4 h.

6.3.3 Precursor synthesis

The synthesis of the cerium glycolate complex, the sodium tris(glycozirconate) complex and alumatrane followed Wongkasemjit's work[21-22]. The cerium glycolate complex was prepared by making a mixture of cerium hydroxide (5.3 mmol of CeO_2), 18 ml of ethylene glycol and 5 mmol of triethylenetetramine with sodium hydroxide at about 12 mol% equivalents to cerium hydroxide. The mixture was magnetically stirred and heated to the boiling point of ethylene glycol for 18 h under N_2. The reaction mixture was cooled overnight under N_2. The precipitated product was filtered and washed with acetonitrile, followed by drying under vacuum.

A similar process was used to synthesize the sodium tris(glycozirconate) complex. Zirconium hydroxide (11.4 mmol of ZrO_2) and approximately 200 mol% sodium hydroxide equivalent to the zirconium dioxide were suspended in 35 ml of ethylene glycol. The reaction mixture was heated under nitrogen in a thermostatted oil bath at 200°C. After 12 h, the solution was virtually clear, indicating reaction completion. The reaction mixture was cooled, and 2-5% of dried methanol in acetonitrile was added. The product precipitated out as a white solid. The solid was filtered off, washed with acetonitrile, and dried under vacuum.

The synthesis of alumatrane was carried out in one step. A mixture of $Al(OH)_3$, TIS and TETA was suspended in EG, and heated to the boiling point of EG

under nitrogen to distill off ethylene glycol along with removal of water liberated from the reaction. The solution was virtually clear, indicating reaction completion. The reaction mixture was cooled at room temperature. The product precipitated out as a white solid. The solid was separated, washed with acetonitrile, and dried under vacuum (0.1 mmHg) at room temperature.

6.3.4 Catalysts Preparation

Cu (25 mol%)-$Ce_{0.6}Zr_{0.4}O_2$ (YY wt %)/Al_2O_3 where YY indicates the amount of Cu (25%)-$Ce_{0.6}Zr_{0.4}O_2$ (0, 10, 20, 30, 40 wt %) relative to Al_2O_3 were prepared by using a sol-gel method at ambient temperature.

Cu (25 mol%)-$Ce_{0.6}Zr_{0.4}O_2$ were prepared using surfactant-aided sol gel technique, which is optimized to produce a single phase CeO_2-ZrO_2 solid solution, fully described in previous study[23]. The Cu (25 mol%)-$Ce_{0.6}Zr_{0.4}O_2$ powders were added to alumatrane in NaOH solution (pH = 10). The content of Cu (25 mol%)-$Ce_{0.6}Zr_{0.4}O_2$ powders ranged from 10, 20, 30, to 40 wt%. Each resulting mixture was stirred till obtaining a gel. The resulting gel was further kept at room temperature for 10 days. The samples were then put in an oven at 110°C for at least 12 h to let them dry before calcination at various temperatures and time.

6.3.5 Catalytic Activity Measurement

The catalytic activity of the CO oxidation for the synthesized samples was evaluated in a differential packed-bed quartz U-tube reactor (ID 6 mm). The inlet gas consisted of 1% CO and 1% O_2 balanced in N_2 with the total flow rate of 30 mL/min corresponding to the space velocity of 10,000 $mLg^{-1}h^{-1}$ and the gas was directly exposed to the 25 mg catalyst as the reactor temperature was stabilized at the reaction temperature without any pretreatment. The reaction temperature was monitored by a thermocouple placed in the middle of the catalyst bed. The effluent gas from the reactor was analyzed by auto-sampling in an on-line gas chromatograph.

6.4 Results and Discussion

Effects of thermal aging on the structural and textural evolution of Al_2O_3 and effects of incorporation of Al_2O_3 with Cu (25 mol%)-$Ce_{0.6}Zr_{0.4}O_2$ at different Cu (25 mol%)-$Ce_{0.6}Zr_{0.4}O_2$ content (0-40 wt%) were investigated by means of powder XRD and N_2 adsorption.

6.4.1 X-ray diffraction (XRD)

Table 6.1 summarizes the structural data obtained for the different calcinations. For the calcination time of 5 h, after the calcination at 1000°C, all the samples display the mixture structure of δ-, θ- and α-Al_2O_3 is observed at 1200°C for all the samples, whereas this high-temperature stable phase exists much more in the pure Al_2O_3 sample than in the mixed samples. Accordingly, the mixture of transition alumina (δ- and θ-Al_2O_3) is better retained in those samples doped with Cu (25 mol%)-$Ce_{0.6}Zr_{0.4}O_2$. While the calcination temperature is increased to 1200°C, these trends become more obvious.

It is seen from Figure 6.1 that the mixture completely converts into corundum structure at 1200°C for the pure Al_2O_3. With a few Cu (25 mol%)-$Ce_{0.6}Zr_{0.4}O_2$ loading, traces of θ-Al_2O_3 are still observed for these samples. For example, the presence of three peaks at $2\theta = 31.25°$, 32.80° and 36.69° correspond to the three strongest lines of monoclinic θ-Al_2O_3. The presence of Cu (25 mol%)-$Ce_{0.6}Zr_{0.4}O_2$ is revealed by the cubic structure of ceria-zirconia mixed oxide. To simulate the harsh conditions that can be met in a CCC, calcination was performed at 1100°C for 24 h. The diffractograms of Cu (25 mol%)-$Ce_{0.6}Zr_{0.4}O_2/Al_2O_3$ samples are presented in Figure 6.2. After calcinations at elevated temperature for this much longer time, all the powders present the predominant corundum phase. There is minor θ-Al_2O_3 phase existing in the samples that have Cu (25 mol%)-$Ce_{0.6}Zr_{0.4}O_2$ $\geq$20 wt%, especially in the Cu (25 mol%)-$Ce_{0.6}Zr_{0.4}O_2$ (20 wt%)/Al_2O_3 sample.

The stabilization of Cu (25 mol%)-$Ce_{0.6}Zr_{0.4}O_2/Al_2O_3$ is synergic in that the presence of the copper-ceria-zirconia hinders the transformation of the transitional aluminas into the α-Al_2O_3. This could be related to the fact that the

CeO_2-ZrO_2 tends to grow as flat two dimensional patches, which prevail over the three-dimensional ones at lower CeO_2-ZrO_2 loadings[24].

The stabilization of Al_2O_3 is also observed when either ZrO_2 or CeO_2 are incorporated with Al_2O_3 (Table 6.1), thin-monolayer dispersion of ZrO_2 was suggested to form over the δ-Al_2O_3 that reconstructed to form bulk ZrO_2 only at very high temperatures, where appreciable migration of surface species can occur; this leads to loss of the interaction between the two phases with a concomitant formation of α-Al_2O_3[25]. The situation appears more complex for CeO_2; in fact some contradictory results have been found as far as textural and structural stabilization of Al_2O_3 by addition of CeO_2 are concerned[26]. At low contents of the impregnated CeO_2, a strong interaction between CeO_2 and Al_2O_3 occurs leading to significant formation of Ce^{3+} species that easily interact at high temperatures, particularly under reducing conditions, leading to formation of patches of $CeAlO_3$. This provides an effective way to prevent support sintering attributed to interfacial structural coherence of $CeAlO_3$ with alumina[26]. Consistently, under oxidizing conditions the stabilizing effect of CeO_2 is less effective, particularly at high loading[27].

It is worth noting that some α-Al_2O_3 is formed in the case of Cu (25%)-CeO_2 (20 wt%)/Al_2O_3 at 1100°C, which is consistent with the high particle size of Cu (25%)-CeO_2 compared to the others (Table 6.2), leading to a minor interface area between the alumina and Cu (25%)-CeO_2 phases.

No evidence for phase separation of the $Ce_{0.6}Zr_{0.4}O_2$ solid solution is found after calcination at 1100°C for 24 h. This is a remarkable result, which indicates that there is a mutual stabilization between the Cu (25%)-$Ce_{0.6}Zr_{0.4}O_2$ and Al_2O_3. Phase diagram indicates that tetragonal ZrO_2-rich and cubic CeO_2-rich are the thermodynamically stable phases at these temperatures[28]. Lack of phase separation could be due to kinetic reasons; however it is reasonable to expect that after calcination at 1100°C for 24 h, equilibrium conditions being attained. We believe that both optimized synthesis conditions leading to a homogeneous solid solution and the mutual stabilization effect are responsible for this high thermal stability of the solid solution.

In addition, the interaction with Al_2O_3 of the Cu (25 mol%)-$Ce_{0.6}Zr_{0.4}O_2$/Al_2O_3 mixed oxides strongly depressed its sintering, as indicated by the

comparison with the average particle size detected in the Cu (25 mol%)-$Ce_{0.6}Zr_{0.4}O_2$ (Table 6.2). This could be attributed either to a synergic stabilization between the Al_2O_3 and copper-ceria-zirconia phases or to the retarding effect of the Al_2O_3 on the sintering rate of the copper-ceria-zirconia phase.

6.4.2 BET measurement

Change of surface areas of pure Al_2O_3 and Cu (25%)-$Ce_{0.6}Zr_{0.4}O_2$ (10-40 wt%)/Al_2O_3 samples due to calcinations is shown in Figure 6.3. For the calcination time of 5 h, the surface area is decreased with increasing calcination temperature from 1000 up to 1200°C; a significant decrease in surface area is displayed at 1200°C for the whole samples. It is also observed that pure Al_2O_3 loses its specific surface area at higher rate than those of Cu (25 mol%)-$Ce_{0.6}Zr_{0.4}O_2$/Al_2O_3 mixed oxides samples. After calcinations at 1200°C, by comparison with the greatly decreased surface area of the pure Al_2O_3 (20 m^2g^{-1}), the mixture retains its surface area to some extent (about 30 m^2g^{-1}) for Cu (25 mol%)-$Ce_{0.6}Zr_{0.4}O_2$/Al_2O_3 (10 and 20 wt%)/Al_2O_3 mixed oxides samples. The higher Cu (25 mol%)-$Ce_{0.6}Zr_{0.4}O_2$ content samples show a lower surface area, which is caused by the relatively much lower surface area of Cu (25 mol%)-$Ce_{0.6}Zr_{0.4}O_2$ than transition aluminas. This trend compromises an improved thermal durability of transition aluminas beyond initial surface area loss when it is added with Cu (25 mol%)-$Ce_{0.6}Zr_{0.4}O_2$ mixed oxides.

Considering the samples aged at 1100°C for various calcinations times (5 and 24 h), it was found that the Cu (25 mol%)-$Ce_{0.6}Zr_{0.4}O_2$/Al_2O_3 samples tend to lose less surface area compared to the pure Al_2O_3, which is obvious especially for samples under 24 h calcination time. As can be seen in Figure 6.3, after the initial drop (5 h), the surface area of Cu (25 mol%)-$Ce_{0.6}Zr_{0.4}O_2$/Al_2O_3 remains at an acceptable stability for a considerable period of calcination time (24 h) at such an elevated temperature. For example, the surface area of the Cu (25 mol%)-$Ce_{0.6}Zr_{0.4}O_2$/Al_2O_3 (28 m^2g^{-1}) loses within 53% of its value from 5 h to as long as 24 h of calcination time, whereas it deteriorates nearly 76% of its value from 5 to 24 h for the pure Al_2O_3 (17 m^2g^{-1}). Meanwhile, the apparent surface area of mixture further decreased as more Cu (25 mol%)-$Ce_{0.6}Zr_{0.4}O_2$ is introduced (30 and 40 wt%).

It can be concluded in this case that the optimum stabilizing effect on transition aluminas is achieved when the doping content of Cu (25 mol%)-$Ce_{0.6}Zr_{0.4}O_2$ increases up to 20 wt%. The effect of Cu (25 mol%)-$Ce_{0.6}Zr_{0.4}O_2$ on transition phases is held with more doping content, whereas the surface area of the whole samples decreases as a result of the dramatically decreased of Cu (25 mol%)-$Ce_{0.6}Zr_{0.4}O_2$ mixed oxides surface area after aging.

6.4.3 Temperature programmed reduction (TPR)

The maximum of the thermal stabilization is achieved for the Cu (25 mol%)-$Ce_{0.6}Zr_{0.4}O_2/Al_2O_3$, the redox properties of this sample was therefore examined in detail. Before commenting on these results, let us recall that the TPR profiles of supported CuO species appeared quite sensitive on the conditions of catalyst preparation[29]. Two reduction peaks, designated as β (197°C) and γ (247°C) were distinguished for a CuO/Al_2O_3 system[30]. The β-peak is attributed to the reduction of isolated Cu^{2+} ions and small two- and three-dimensional clusters, whereas the γ -peak is attributed to the reduction of large three-dimensional clusters and bulk phase.

As far as the reduction of CeO_2 is concerned, the TPR profiles of high surface area samples feature a reduction profile, which is characterized by two reduction peaks (300-600°C and 700-1000°C). These are due, respectively, to reduction of surface (or nanocrystalline) and bulk CeO_2; the insertion of ZrO_2 into the CeO_2 lattice with formation of a solid solution modifies the TPR profiles, leading to essentially a single reduction feature centered at about 427-627°C[31].

Reduction of CuO supported on CeO_2, CeO_2-ZrO_2 and ZrO_2 started above 100°C[32-33]. In pure CuO this occurred above 250°C. At least 2 to 3 reduction peaks were observed in the supported catalysts, indicating the existence of different type of CuO species.

The TPR profiles of the Cu (25%)-$Ce_xZr_{1-x}O_2$ (20 wt%)/Al_2O_3 samples are shown in Figure 6.4. Cu (25%)-ZrO_2 (20 wt%)/Al_2O_3 showed overlapping reduction peaks at 177 and 192°C. These peaks in Cu (25%)-CeO_2 (20 wt%)/Al_2O_3 appeared at lower temperatures, 152 and 172°C, respectively. In Cu (25

mol%)-$Ce_{0.6}Zr_{0.4}O_2$ (20 wt%)/Al_2O_3, they occurred at still lower temperatures, 125 and 162°C, respectively. With different supports, the reducibility of copper increased in the order $ZrO_2/Al_2O_3 < CeO_2/Al_2O_3 < CeO_2$-$ZrO_2/Al_2O_3$.

TPR of copper-ceria-zirconia mixed oxides was investigated by our previous work[23]. The results indicated that there are three copper species in the catalysts; namely, the finely dispersed CuO, the copper ion in the solid solution, and the bulk CuO. Two reduction peaks of finely dispersed CuO and the copper ion in the solid solution were observed at below 200°C and the reduction peak of bulk CuO can be observed at approximately 270°C. The TPR peaks for our catalysts (Figure 6.4) reveal that the latter type of CuO particles is not present in our catalyst samples.

6.4.4 CO oxidation

The comparison of the CO oxidation catalytic activities of catalysts after calcinations for 5 h at 800°C indicated in Figure 6.5. This heat treatment temperature (800°C) corresponds to the moderate thermal conditions of practical automotive exhaust gases[34]. The activities of the $Ce_{0.6}Zr_{0.4}O_2$ and pure CeO_2 were quite low. Pure ZrO_2 and CuO had no catalytic activity under present condition (not shown), however, Cu (25 mol%)-$Ce_{0.6}Zr_{0.4}O_2$ (20 wt%)/Al_2O_3 showed much higher catalytic activity. The enhancement of the catalytic activity of the catalysts should be attributed to a synergistic effect between CuO and the supports. The ''light-off'' temperatures (T_{100}) for 100% CO conversion over the Cu (25%)-CeO_2 (20 wt%)/Al_2O_3 and Cu (25 mol%)-$Ce_{0.6}Zr_{0.4}O_2$ (20 wt%)/ Al_2O_3 catalysts were 160 and 180°C, respectively. The maximal CO conversion on the Cu (25%)-ZrO_2 (20 wt%)/Al_2O_3 was only 88% in this work.

Luo et al.[35] and the results from our previous work[23] suggested that dispersed CuO was responsible for the high CO oxidation catalytic activity and the bulk CuO may deteriorate the catalytic activity[36]. According to the TPR analyses, the Cu (25%)-CeO_2 (20 wt%)/Al_2O_3 had the highest CuO dispersion degree and the dispersion degree of CuO decreased with the increase of Zr content.

The result from Figure 6.5 showed that the Cu (25%)-CeO_2 (20 wt%)/Al_2O_3 catalyst exhibited the highest catalytic activity and the ''light-off'' temperature of Cu (25%)-CeO_2 (20 wt%)/Al_2O_3 catalyst was about 20°C lower than

that of the Cu (25 mol%)-$Ce_{0.6}Zr_{0.4}O_2$ (20 wt%)/Al_2O_3 catalyst. For comparison, the Cu (25%)-CeO_2 (20 wt%)/Al_2O_3 and Cu (25 mol%)-$Ce_{0.6}Zr_{0.4}O_2$ (20 wt%)/Al_2O_3 catalysts were further investigated. The catalytic activities for CO oxidation of Cu (25%)-CeO_2 (20 wt%)/Al_2O_3 and Cu (25 mol%)-$Ce_{0.6}Zr_{0.4}O_2$ (20 wt%)/Al_2O_3 catalysts calcined at harsh conditions that can be met in a CCC (1100°C/24 h) are also presented in Figure 6.5. It can be seen that the catalytic activity of the Cu (25%)-CeO_2 (20 wt%)/Al_2O_3 decreased, which may be due to the sinter of the catalyst and the formation of bulk CuO at higher temperature. The CO conversion of the Cu (25%)-CeO_2 (20 wt%)/Al_2O_3 catalyst calcined at 1100°C for 24 h was only about 70% when the reaction temperature reached 220°C. The T_{100} of the Cu (25 mol%)-$Ce_{0.6}Zr_{0.4}O_2$ (20 wt%)/Al_2O_3 catalysts calcined 1100°C for 24 h was 220°C. Compared with the Cu (25 mol%)-$Ce_{0.6}Zr_{0.4}O_2$ (20 wt%)/Al_2O_3, the Cu (25%)-CeO_2 (20 wt%)/Al_2O_3 catalyst exhibited higher catalytic activity when the calcination temperature was lower than 1100°C. But when they were calcined at 1100°C, the result was just the opposite. This may indicate that incorporating zirconium into CeO_2 can improve the thermal resistance of the resulting mixed oxide, which makes Cu (25 mol%)-$Ce_{0.6}Zr_{0.4}O_2$ (20 wt%)/Al_2O_3 catalyst have better thermal resistance than Cu (25%)-CeO_2 (20 wt%)/Al_2O_3 catalyst. The similar result was also reported in our previous work[37-38]. By catalytic activity tests, it was noted that the catalytic activities of the catalysts for CO oxidation decreased with increasing Zr content, which may be due to the decrease of the CuO dispersion degree on the surface of the supports. This can be identified by the TPR analyses. However, incorporating zirconium into CeO_2 can improve the thermal resistance of the resulting mixed oxide, which makes the Cu (25 mol%)-$Ce_{0.6}Zr_{0.4}O_2$ (20 wt%)/Al_2O_3 catalyst have better thermal resistance than Cu (25%)-CeO_2 (20 wt%)/Al_2O_3 catalyst at higher temperature.

It can be concluded from the results of catalytic activity tests that the Cu (25%)-CeO_2 (20 wt%)/Al_2O_3 catalyst showed better catalytic activity than the Cu (25 mol%)-$Ce_{0.6}Zr_{0.4}O_2$ (20 wt%)/Al_2O_3 catalyst at lower temperature, but the catalytic activity of Cu (25%)-CeO_2 (20 wt%)/Al_2O_3catalyst decreased more rapidly than that of Cu (25 mol%)-$Ce_{0.6}Zr_{0.4}O_2$ (20 wt%)/Al_2O_3 catalyst when the calcination temperature increased to 1100°C.

6.5 Conclusions

The introduction of Cu (25 mol%)-$Ce_{0.6}Zr_{0.4}O_2$ mixed oxides into alumina causes a decelerating effect on its phase transformation and retains a certain surface area for a long period of time at elevated temperature beyond initial quick loss of surface area. When the Cu (25 mol%)-$Ce_{0.6}Zr_{0.4}O_2$ content is less than 20%, it shows a slightly suppressing effect on the transformation temperature. When 20% Cu (25 mol%)-$Ce_{0.6}Zr_{0.4}O_2$ is added, the mixed powders maintain an optimized stability, with an acceptable specific surface area of 30 m^2g^{-1} after calcinations at 1200°C for 5 h. When more Cu (25 mol%)-$Ce_{0.6}Zr_{0.4}O_2$ is further added, the surface area of the mixed powders decreases again due to the much lower surface area of Cu (25 mol%)-$Ce_{0.6}Zr_{0.4}O_2$ itself after such a long period of time at elevated temperature. This phenomenon may be expressed by the decomposition of Cu (25 mol%)-$Ce_{0.6}Zr_{0.4}O_2$ mixed oxides, which may decrease the surface diffusion and rate of sintering of alumina. Furthermore, the introducing of Cu (25 mol%)-$Ce_{0.6}Zr_{0.4}O_2$ additives causes less particle-to-particle contacts in the alumina bulk, which also may retard the grain growth and finally the transformation.

In the CO oxidation reaction, the CeO_2 (20 wt%)/Al_2O_3 catalyst exhibited the highest catalytic activity. However, incorporation of zirconium into CeO_2 can improve the thermal resistance of the catalyst. The Cu (25 mol%)-$Ce_{0.6}Zr_{0.4}O_2$ (20 wt%)/Al_2O_3 catalyst had better catalytic property than CeO_2 (20 wt%)/Al_2O_3 catalyst when they were both calcined at 1100°C for 24 h. The results of TPR analyses that the dispersed CuO was responsible for the high catalytic activity of CO oxidation.

6.6 Acknowledgments

The authors gratefully acknowledge the financial support of the Postgraduate Education and Research Program in Petroleum and Petrochemical Technology, Thailand, the PPT Consortium (ADB) Fund, Thailand, and the Ratchadapisake Sompote Fund, Chulalongkorn University. Special thanks go to Mr. Robert Wright for the English proofreading.

6.7 References

1) Taylor, K. C. Automobile catalytic converters. In Catalysis:Science and Technology; Anderson, J. R., Boudart, M., Eds.; Springer-Verlag: Berlin, 1984; vol. 5, pp 119-170.
2) Bertelsen, B. I. Platinum Met. Rev. 2001, 45, 50.
3) A. Obuchi, A. Ohi, M. Nakamura, A. Ogata, K. Mizuno, H. Ohuchi, Appl. Catal. B 2 (1993) 71.
4) V.I. Parvulescu, P. Grange, B. Delmon, Catal. Today 46 (1998) 233.
5) R.T. Rewick, H. Wise, J. Catal. 40 (1975) 301.
6) Hummer JK. Prog. Energy Combust. Sci. 1980; 6: 177.
7) Martínez-Arias A, Fernández-García M, Soria J, Conesa JC. J. Catal. 1999; 182: 367.
8) Ka˘Spar J, Fornasiero P, Graziani M. Catal. Today 1999; 50: 285.
9) F. Zamar, A. Trovarelli, C. de Leitenburg, G. Dolcetti, Stud. Surf. Sci. Catal. 101 (1996) 1283.
10) M. Pijolat, M. Prin, M. Soustelle, O. Touret, P. Nortier, J. Chem. Soc. Faraday Trans. 91 (1995) 3941.
11) F. Zamar, A. Trovarelli, C. de Leitenburg, G. Dolcetti, J. Chem. Soc. Chem. Comm. (1995) 965.
12) Y. Sun, P.A. Sermon, J. Mater. Chem. 6 (1996) 1025.
13) M.H. Yao, R.J. Baird, F.W. Kunz, T.E. Hoost, J. Catal. 166(1997) 67.
14) T. Masui, K. Fujiwara, Y.M. Peng, K. Machida, G.Y. Adachi, Chem. Lett. (1997) 1285.
15) R. Di Monte, J. Kaspar, P. Fornasiero, A. Ferrero, G. Gubitosa, M. Graziani, Stud. Surf. Sci. Catal. 116 (1998) 559.
16) H.C. Yao, Y.F. Yu Yao, J. Catal. 86 (1984) 254.
17) J.Z. Shyu, W.H. Weber, H.S. Gandhi, J. Phys. Chem. 92(1988) 4964.
18) M.H. Yao, R.J. Baird, F.W. Kunz, T.E. Hoost, J. Catal. 166 (1997) 67.
19) Fernandez-Garcia, M.; Martinez-Arias, A.; Hungria, A. B.; Iglesias-Juez, A.; Conesa, J. C.; Soria, J. Phys. Chem. Chem. Phys. 2002, 4, 2473.

20) Fernandez-Garcia, M.; Martinez-Arias, A.; Iglesias-Juez, A.; Belver, C.; Hungria, A. B.; Conesa, J. C.; Soria, J. J. Catal. 2000, 194, 385.

21) Ksapabutr B, Gulari E, Wongkasemjit S, Mater. Chem. and Phy. 83(2004) 34.

22) Ksapabutr B, Gulari E, Wongkasemjit S, Colloids and Surfaces A: Physicochem. Eng. Aspects 233 (2004) 145.

23) Rumruangwong, M.; Wongkasemjit, S., Journal of the American Ceramic Society, Submitted.

24) M. Fernandez Garcia, A. Martinez Arias, A. Iglesias Juez, C. Belver, A.B. Hungria, J.C. Conesa, J. Soria, J. Catal. 194(2000) 385.

25) Horiuchi, T.; Teshima, Y.; Osaki, T.; Sugiyama, T.; Suzuki, K.; Mori, T. Catal. Lett. 1999, 62, 107.

26) Piras, A.; Trovarelli, A.; Dolcetti, G. Appl. Catal., B 2000, 28, L77.

27) Oudet, F.; Bordes, E.; Courtine, P.; Maxant, G.; Lambert, C.; Guerlet, J. P. Stud. Surf. Sci. Catal. 1987, 30, 313.

28) E. Tani, M. Yoshimura, S. Somiya, J. Am. Ceram. Soc. 66(1983) 506.

29) M.F. Luo, Y.J. Zhong, X.X. Yuan, X.M. Zheng, Appl. Catal. A Gen.162 (1997) 121.

30) W.P. Dow, Y.P. Wang, T.J. Huang, J. Catal. 160 (1996) 155.

31) Ranga Rao G. Bull. Mater. Sci. 1999; 22: 89.

32) M.-F. Luo, Y.-J. Zhong, X.-X. Yuan, X.-M. Zheng, Appl. Catal. A 162(1997) 121.

33) G. Avgouropoulos, T. Ioannides, Appl. Catal. A 244 (2003) 155.

34) M. Ozawa*, K. Matuda, S. Suzuki, Journal of Alloys and Compounds 303–304 (2000) 56–59

35) Luo M-F, Hou Y-Y, Yuan X-X, Zheng X-M (1998) Catal Lett 50:205

36) Wang S-P, Wang X-Y, Huang J, Zhang S-M, Wang S-R, Wu S-H (2007) Catal Commun 8:231

37) Rumruangwong, M.; Wongkasemjit, S. (2008), Applied Organometallic Chemistry 22: 1-4.

38) Rumruangwong, M.; Wongkasemjit, S. (2006), Applied Organometallic Chemistry 20: 615-625.

Table 6.1 Powder X-rays diffraction results of the copper-ceria-zirconia mixed alumina calcined at different conditions

Sample	T (°C)	Time (h)	Phases
Al_2O_3	1000	5	δ- and θ-Al_2O_3
	1100	5	δ-, θ- and α-Al_2O_3
	1200	5	α-Al_2O_3
	1100	24	α-Al_2O_3
Cu (25 mol%)-$Ce_{0.6}Zr_{0.4}O_2$ (10 wt%)/Al_2O_3	1000	5	δ- and θ-Al_2O_3+CZ
	1100	5	δ- and θ-Al_2O_3+CZ
	1200	5	θ- and α-Al_2O_3+CZ
	1100	24	α-Al_2O_3+CZ
Cu (25 mol%)-$Ce_{0.6}Zr_{0.4}O_2$ (20 wt%)/Al_2O_3	1000	5	δ- and θ-Al_2O_3+CZ
	1100	5	δ- and θ-Al_2O_3+CZ
	1200	5	θ- and α-Al_2O_3+CZ
	1100	24	θ- and α-Al_2O_3+CZ
Cu (25 mol%)-$Ce_{0.6}Zr_{0.4}O_2$ (30 wt%)/Al_2O_3	1000	5	δ- and θ-Al_2O_3+CZ
	1100	5	δ- and θ-Al_2O_3+CZ
	1200	5	θ- and α-Al_2O_3+CZ
	1100	24	θ- and α-Al_2O_3+CZ
Cu (25 mol%)-$Ce_{0.6}Zr_{0.4}O_2$ (40 wt%)/Al_2O_3	1000	5	δ- and θ-Al_2O_3+CZ
	1100	5	δ- and θ-Al_2O_3+CZ
	1200	5	θ- and α-Al_2O_3+CZ
	1100	24	θ- and α-Al_2O_3+CZ
Cu (25 mol%)-CeO_2 (20 wt%)/Al_2O_3	1000	5	δ- and θ-Al_2O_3+CeO_2
	1100	5	θ- and α-Al_2O_3+CeO_2
	1200	5	θ- and α-Al_2O_3+CeO_2
	1100	24	θ- and α-Al_2O_3+CeO_2
Cu (25 mol%)-ZrO_2 (20 wt%)/Al_2O_3	1000	5	δ- and θ-Al_2O_3+ZrO_2
	1100	5	δ- and θ-Al_2O_3+ZrO_2
	1200	5	θ- and α-Al_2O_3+ZrO_2
	1100	24	θ- and α-Al_2O_3+ZrO_2

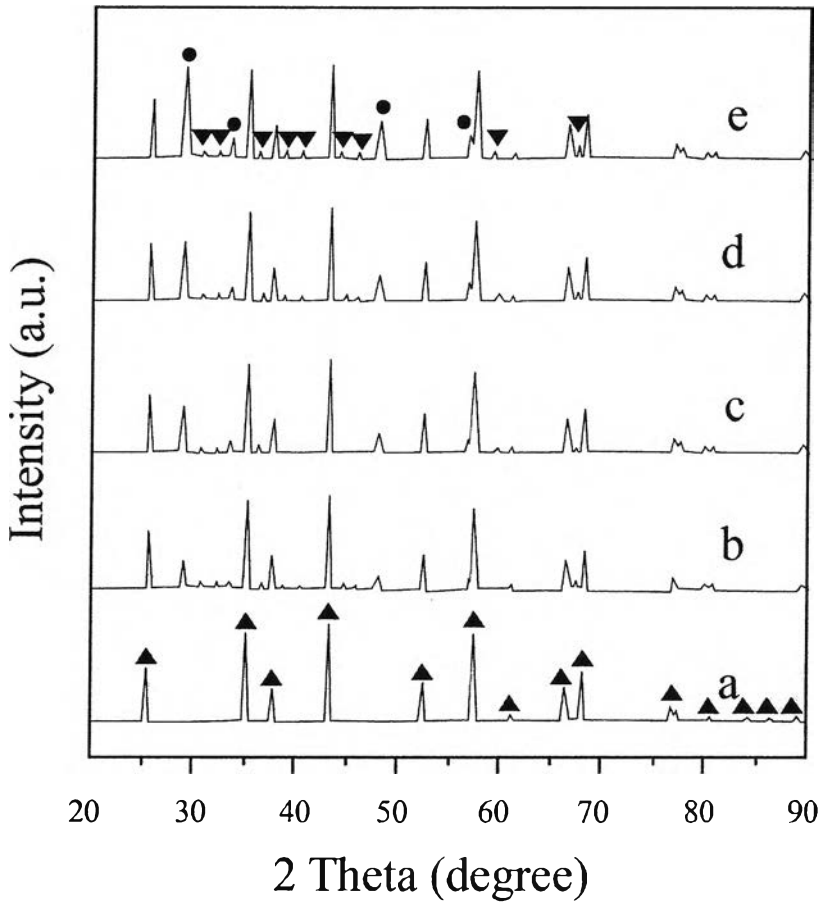

Figure 6.1 X-ray diffractograms of mixed oxides calcined at 1200°C for 5 h. (a) The pure alumina and various Cu (25 mol%)-$Ce_{0.6}Zr_{0.4}O_2$ content: (b) 10%; (c) 20%;(d) 30%; and (e) 40%.

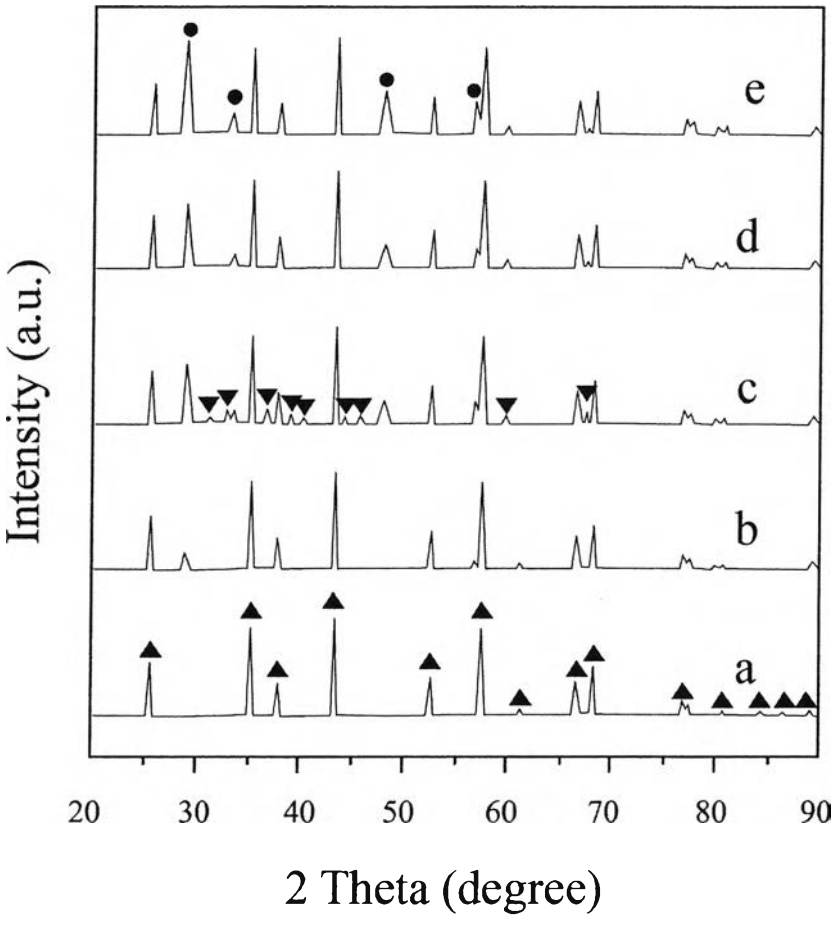

Figure 6.2 X-ray diffractograms of mixed oxides calcined at 1100°C for 24 h. (a) The pure alumina and various Cu (25 mol%)-$Ce_{0.6}Zr_{0.4}O_2$ content: (b) 10%; (c) 20%;(d) 30%; and (e) 40%.

Table 6.2 Effect of aging condition on the particle size of copper-ceria-zirconia mixed oxides.

Sample	T (°C)	Time (h)	ceria-zirconia mixed oxide Particle size (nm)
Cu (25 mol%)-CeO_2 (20 wt%)/Al_2O_3	1000	5	15
	1100	5	20
	1200	5	28
	1100	24	31
Cu (25 mol%)-ZrO_2 (20 wt%)/Al_2O_3	1000	5	6
	1100	5	10
	1200	5	14
	1100	24	15
Cu (25 mol%)-$Ce_{0.6}Zr_{0.4}O_2$ (20 wt%)/Al_2O_3	1000	5	5
	1100	5	9
	1200	5	11
	1100	24	12
Cu (25 mol%)-$Ce_{0.6}Zr_{0.4}O_2$	1000	5	20
	1100	5	26
	1200	5	31
	1100	24	35

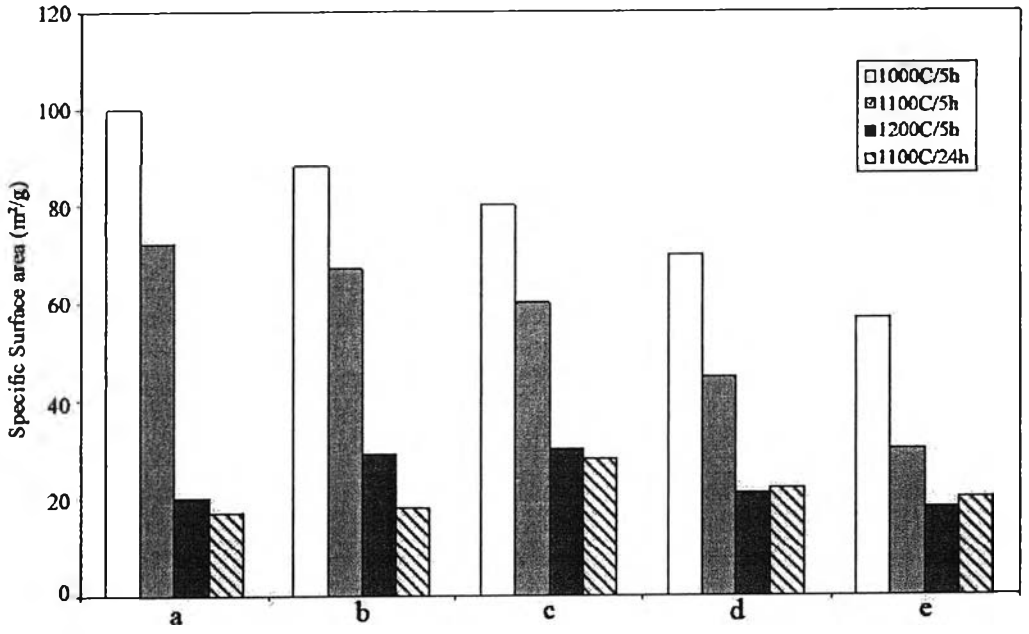

Figure 6.3 Surface area of mixed oxides calcined at different conditions (a) The pure alumina and various Cu (25 mol%)-$Ce_{0.6}Zr_{0.4}O_2$ content: (b) 10%; (c) 20%;(d) 30%; and (e) 40%.

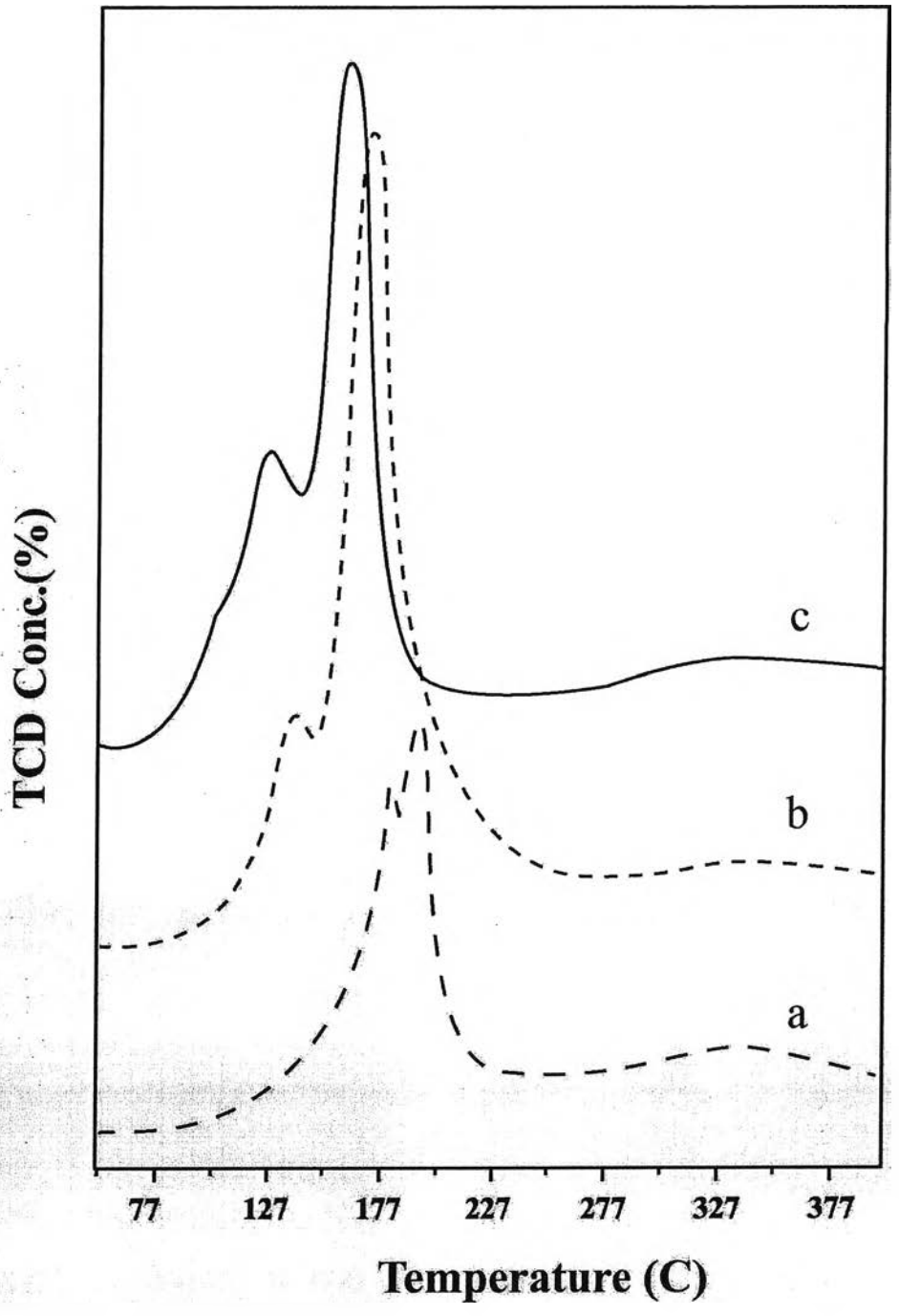

Figure 6.4 TPR profiles for mixed oxides (a) Cu (25 mol%)-ZrO_2 (20 wt%)/Al_2O_3; (b) Cu (25 mol%)-CeO_2 (20 wt%)/Al_2O_3; (c) Cu (25 mol%)-$Ce_{0.6}Zr_{0.4}O_2$ (20 wt%)/Al_2O_3.

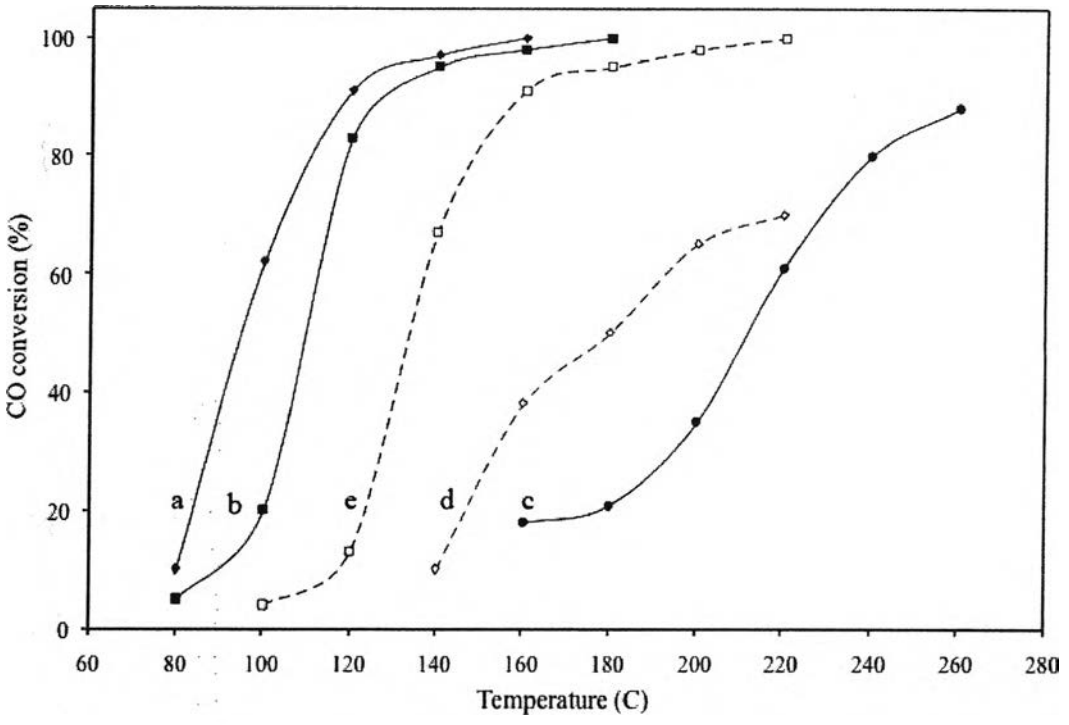

Figure 6.5 Catalytic activities of CO oxidation over mixed oxides calcined at 800°C for 5 h (a) Cu (25 mol%)-CeO_2 (20 wt%)/Al_2O_3; (b) Cu (25 mol%)-$Ce_{0.6}Zr_{0.4}O_2$ (20 wt%)/Al_2O_3; (c) Cu (25 mol%)-ZrO_2 (20 wt%)/Al_2O_3 and mixed oxides calcined at 1100°C for 24 h (d) Cu (25 mol%)-CeO_2 (20 wt%)/Al_2O_3; (e) Cu (25 mol%)-$Ce_{0.6}Zr_{0.4}O_2$ (20 wt%)/Al_2O_3.